SPE 109162

Integrated Wellbore/Reservoir Dynamic Simulation

Bin Hu, SPE, SPT Group; Jan Sagen, IFE; Gaël Chupin, SPE, Tor Haugset, SPT Group; Arild Ek, IFE; Tor Sommersel, Zheng Gang Xu, SPE, Juan Carlos Mantecon, SPE, SPT Group

This paper was prepared for presentation at the 2007 SPE Asia Pacific Oil & Gas Conference and Exhibition held in Jakarta, Indonesia, 30 October–1 November 2007.

Abstract

A comprehensive dynamic wellbore/reservoir flow model is successfully built by implicitly coupling a wellbore flow model with a near-wellbore reservoir model. The integrated model can be used to simulate various well flow transients that are subject to wellbore/reservoir dynamic interactions.

In order to evaluate its performance, several hypothetic cases, such as well shut-in/start-up, heading, coning, and crossflow, are simulated. Comparison is made between the integrated approach and the conventional IPR approach, and the advantage of using the integrated model is justified.

With given completion details and early-time reservoir data, the integrated model is then used to simulate a pressure buildup and drawdown test of an appraisal gas well. The simulation results show that the model can easily and accurately match the well testing data only by tuning the skin factor, which indicates the integrated model is suitable for optimizing well testing design, assisting well testing interpretation, and estimating the BHP where downhole measurements are not cost-effective and reliable.

Introduction

Conventional dynamic well flow models use steady-state IPRs to describe the influx of oil and gas from the reservoir, which ignore the flow transients in the near-wellbore area. On the other hand, reservoir models use steady-state lift curves to represent the TPRs, which ignore the flow dynamics in the wellbore. Neither the well models nor the reservoir models can account for the dynamic wellbore/reservoir interactions. For example, Gaspari[1] *et al*. verified the performance of an advanced transient multiphase flow model with the field data from an offshore well in Brazil. Even though the simulation matched the steady-state production perfectly, the model failed to simulate the shut-in/start-up operation by a big deviation in the downhole shut-in pressure prediction. This was attributed to the strong pressure transient in the tight reservoir, which was not considered in the modeling.

To bridge this modeling gap, many efforts[2~15] have been made in developing integrated transient wellbore/reservoir models. These modeling efforts were related to the simulation of well testing[2,4,6,7,8,10,11,15], heavy oil thermal recovery[5], long horizontal well performance[3,9], and unstable well flows[12,13,14]. Despite most of the models have been very successful in simulating the special cases that they were developed for, they are lack of the general applicability for being used in a much wider scope due to either a poor wellbore flow model was used, or a simple reservoir description was adopted, or the numerical coupling between the wellbore and reservoir models was not properly handled.

For example, one of the latest efforts from Ballard[14] *et al.* was intended to couple a comprehensive well flow model with a comprehensive reservoir model for investigating formation heading and liquid loading in a gas well that produces from a fractured tight reservoir. The coupled system is really advanced in terms of the modeling capabilities of the wellbore and reservoir models. However, the simulation speed had to be kept very slow in order to assure the coupling numerical stability, which was based on an explicit procedure.

Some previous modeling efforts tried to solve the whole wellbore/reservoir system in one unified numerical scheme that could skip the coupling issues between the two models. This can only be achieved by sacrificing the modeling details of either the wellbore or the reservoir, e.g. by attaching an analytical solution of the reservoir model to the wellbore flow model, or by attaching a simple wellbore model to the reservoir model. However, this approach is not practical when the models on both sides of the sandface need to be comprehensive, particularly, when they are made to deal with the complexity of the modern advanced wells. The multiphase flow in wellbore and in porous medium is fundamentally different in nature, which requires separate modeling formulations and different numerical solution schemes.

This paper is concerned with the development and testing of a novel integrated wellbore/reservoir model, which is achieved by implicitly coupling an existing transient wellbore flow model with an existing near-wellbore reservoir model. As both the two models are already comprehensive and powerful in their functionalities, the main focus of this work is on the numerical coupling between the two models and testing the usability of the integrated simulator. The detailed introduction of the models and their integration are given below.

Development of the integrated model

The development of the integrated simulator consists of three phases. First, two flow models, one for wellbore and one for reservoir, have to be selected. Second, the two models must be integrated to allow exchanging pressure and flow information at the sandface. Third, the simulator based on the integrated model has to be made easy and flexible to use.

Description of the wellbore model

A commercial available transient multiphase flow model described by Bendiksen[16] *et al.* is selected for modeling the wellbore flow. The performance of the model has been extensively verified against both laboratory and field data as shown by Nossen[17] *et al*. The same model was also selected by Ballard[14] *et al.* for integration with an in-house reservoir simulator. When being selected in this work, most of the latest developments of the model are included.

The selected model is now a three-fluid model compared with the early version given by Bendiksen[16] *et al.*, which is capable of simulating transient three-phase gas-oil-water flow in pipes. At each time step, a set of five coupled mass conservation equations are solved for, respectively, the gas phase, the water droplets, the oil droplets, the oil film and the water film. Three momentum equations are solved for respectively the gas/droplet field, the oil bulk, and the water bulk. The model is closed by an appropriate set of closure laws describing the friction at the wall and the fluid interface, the droplet and bubble entrainment, and the droplet deposition. One single energy balance equation is solved for the fluid mixture.

In well flow simulation applications, the model is capable of modeling the complicated well trajectory such as a “snake” well, the advanced well completion such as a smart well, and the characteristics of various well equipment such as valves and pumps. The model also has a strong heat transfer calculation function that can account for the transient heat transfer between the tubing and the annulus, and between the annulus and the formation. In addition, the frictional cooling/heating of the flow in the wellbore, and the Joule-Thomson effect of the flow from the reservoir to the wellbore are also considered in the model.

Description of the near-wellbore reservoir model

An in-house reservoir model is selected to model the flow in the near-wellbore area. Sagen[18] *et al.* has already given the details of the model in a separate publication. The model is capable of simulating three-phase Darcy flow in porous medium. The flow equations are solved in three dimensions, giving saturations and pressures varying in space and time as output in addition to the flow rate of each phase at the boundary. Standard industry file formats are used for output.

The model supports both radial and rectangular grid. The numerical and physical kernel code is not affected by the choice of grid. The flow and thermal equations of the model are solved fully implicitly, using the Newton-Raphson iterative method at each time step.

Input data to the model are permeability and porosities of the porous medium, fluid transport properties, and thermal properties of the rock and fluids. Boundary conditions at the well and at the outer reservoir must be given. Typical time-dependent boundary conditions are injection/production flow rates, pressure and temperature. Initial condition including the pressure and saturation for each phase at each numerical block must be defined prior to simulation. The model also reserves the skin option for the situation when the inflow deviation from its ideal can not be properly accounted for by the reservoir model itself, e.g. the perforation skin.

The simulation input information is stored in a keyword based text file. The format of this input file is made simple in order to facilitate the data transfer from other reservoir simulators. For example, Chupin[18] *et al.* has demonstrated the feasibility of automatically transferring the simulation snapshots from another reservoir simulator into this reservoir model as the input information that contains the boundary and initial conditions for the selected near-wellbore domain of interest.

Model integration

The reservoir model is considered as a plug-in to the wellbore model, and the integrated simulation is fully controlled by the wellbore model. During the simulation, the wellbore model provides the pressure boundary to the reservoir model and the reservoir model calculates the flow rate of each phase at the interface.

The flow rates can be positive or negative depending on the flow directions corresponding to production and injection respectively. In case of injection or back seepage, the phase mass fractions in the wellbore section that the reservoir model interfaces to are converted to saturations in order to calculate the fractional injection rate for each phase.

The numerical coupling between the two models is implemented in an implicit scheme. The concept of the implicit coupling here is that the reservoir model calculates a sensitivity coefficient for the production rate with respect to the wellbore pressure at each time step and makes it available for the wellbore flow model. At the next time step, the wellbore model uses this sensitivity coefficient to solve the new wellbore pressure. The sensitivity coefficient is extracted from the Jacobian matrix of the reservoir model at the last iteration. The size of the near-wellbore domain contributing to the rate-pressure sensitivity calculation is determined by the coupling level that can be specified as a simulation input.

The principle of the implicit coupling can be summarized as follows:

1. Assuming the models have been integrated up to time step *n*, the wellbore model begins integration to time step *n+1* by requesting the reservoir model to calculate the sensitivity coefficients a_P^n and b_P^n, which are used in the relation below:
$$M_P^{n+1} = a_P^n P_P^{n+1} + b_P^n$$
where P_P is the pressure in the wellbore, M_P is the mass flow rate for each phase and the subscript *p* refers to a given phase, i.e. gas, oil or water.
2. The wellbore model uses the above relation as a boundary condition and solves for the complete wellbore. The wellbore model has now completed time step *n+1* and sends P_P^{n+1} and M_P^{n+1} to the reservoir model.

3. The reservoir model completes its time step *n+1* calculation by using the wellbore model supplied boundary condition.

The sensitivity coefficient a_P^n is calculated by

$$a_P^n = \frac{dM_P^n}{dP_P^n}$$

which can be analytically derived from the reservoir model equations given by Sagen[18] *et al.*

b_P^n is simply given by

$$b_P^n = M_P^n - a_P^n P_P^n$$

With this implicit coupling implementation, the integrated model can run simulation in relative large time steps while maintaining the numerical stability. From the testing experiences so far, the simulation speed is less an issue for all the tested cases described in this paper.

PVT and simulation flexibilities

The fluid PVT properties used in the simulation are pre-calculated and stored in a table as a function of pressure and temperature. During the simulation, both the wellbore model and the reservoir model look up the table to get the fluid properties by interpolation. As the same table is used for both models, it secures the PVT consistence across the sandface. Otherwise, if different PVT solution is used, even a slight difference in fluid physical properties, e.g. the densities, can easily trigger simulation crash. Particularly for the well shut-in simulation, when the same fluid flows back and forth across the sandface, the volume error can accumulate and result in pressure integration excursion due to density difference.

The simulation with the integrated model is made flexible in terms of initial conditions used by the wellbore model and the reservoir model. For example, both two models can either use the initial condition specified by the user, or use the simulation snapshot from a previous run as the initial condition. In fact, the snapshot is not necessary from a previous integrated simulation. It can be from standalone simulation of the two models.

This treatment significantly improves the simulation efficiency. For example, the user can very quickly run the reservoir simulation standalone into a condition that is of interest to be coupled with the wellbore model for further simulation. Otherwise, if the two models have to be coupled from the very beginning, then it may take very long simulation time before the reservoir enters into the scenario of interest. This is due to that the integrated run always chooses the smaller integration time step of the two models, which inevitably slow down the simulation speed compared with running the two models in a separate mode.

Testing of the integrated simulator

Several hypothetic cases are simulated using the integrated model. As the dynamic phenomena of the selected cases are already of our common knowledge, they can be used as benchmarks to qualitatively verify the performance of the integrated model. The simulation results are presented below without giving too many details on the inputs since the cases are hypothetic and have no quantitative significance here.

Case 1: well shut-in/start-up

Table 1 lists the main parameters used for a well shut-in/start-up simulation based on a cylindrical reservoir. The simulation results are given in Figure 1 with both the BHP and the sandface mass flow rate. There is no gas presence in the reservoir as the BHP is kept higher than the bubble pressure.

The simulation starts from a previous run assuming the well is producing at a steady state. Then at hour 1, the wellhead choke is closed. Figure 1 shows the BHP gradually builds up while the afterflow is decreasing. In this case, it takes almost one hour for the BHP to reach the reservoir pressure. If using an IPR to represent the inflow, the pressure buildup would be faster.

The difference between an IPR approach and the integrated approach can be more clearly illustrated in the start-up simulation. When reopen the wellhead choke at hour 3, the BHP drops immediately and results in a peak flow from the reservoir. If looking at the corresponding BHP, i.e. point A, and the same value after a while, i.e. point B, they should give the same sandface flow rate if an IPR is used as the two points have the same drawdown. However, point A results in a much higher flow rate than point B does when the transient reservoir response is considered, which are marked by A' and B' respectively in the figure. This is due to that the sandface flowrate depends on the local pressure gradient that is at its maximum at the moment of start-up.

To accurately calculate this inflow peak is crucial for some wells, e.g. those equipped with downhole sandscreen. They may collapse if the sudden change of the inflow from the reservoir is too big.

Case 2: gas-lift casing heading

Casing heading is a well-known operation instability for gas-lift wells. When it occurs, lifting gas regularly accumulates and discharges from annulus to tubing and results in severe pressure and flow oscillations. The stability criteria for gas-lift design however do not consider the near-wellbore dynamics, which can often result in an over-conservative gas-lift design. Asheim[20] and Hasan[21] *et al.* were the first who pointed out the importance of near-wellbore dynamics to casing heading.

Case 2 uses the well parameters given in Table 2 to demonstrate the difference when the reservoir dynamics is considered. Figure 2 shows the simulation results. The black curve is the result from integrated model, while the red one is from the same well model but using an IPR to replace the reservoir model. The IPR is tuned to match the simulation of the integrated model at a stable flow when a high gas injection rate is applied. At hour 10, when the gas injection is reduced to a low level, the two simulation mismatches with each other. The oscillation from the IPR approach is much larger than that from the integrated approach. This implies that the near-wellbore reservoir dynamics intend to reduce the instability. Similar observation is also made by Sturm[13] *et al.* when they did the same comparison.

The explanation is that the fast response of sandface flow rate with respect to the change of BHP (as shown in Case 1) can slow down the snowball effect of casing heading. For example, the fast increasing sandface flow will compensate the sudden drop of BHP, therefore, reduces the additional suction of annulus gas that could bring BHP down further.

Case 3: dynamic gas coning

Case 3 is made to simulate the dynamic gas coning process during a start-up. Table 3 gives the parameters used for the modeling. Figure 3 sketches the flow system that is simulated. A is the well, and B is the seabed flowline that has a slight downward profile towards the riser C. The B profile is selected such in order to favor the formation of riser-base slugging in this case.

As shown in Figure 3, the well is perforated to produce the oil zone. Without considering the gas cap, the simulation exhibits an oscillation with a long periodic time and big amplitude as in Figure 4. Since the oil zone is modeled as three numerical layers, Figure 4 gives the sandface oil mass rate for each layer.

However, if including the gas cap in the model, the results are totally different since gas coning can occur on the top oil layer near the wellbore. As Figure 5 shows, the oil production from the top layer is much lower than the other two, which indicates the coning gas occupies the oil flow path in the top layer and reduces the oil production. In the meantime, the coning is still developing after 70 hours from start-up as the general trend of the top layer oil production continues decreasing. The coning gas also increases the total volumetric production and GOR, which intends to reduce the severe slugging by a shorter periodic time in this case.

Case 4: crossflow

Case 4 is intended to show the crossflow between different production zones during the well shut-in. Table 4 is the basic information used in this run. Figure 6 shows the sketch of the simulated well that produces from both an oil zone and a gas zone, assuming no communication between the two zones on the formation side. As given in Table 4, the gas zone pressure is much lower than the oil zone, which implies crossflow from oil zone to gas zone may happen. To magnify the phenomenon, a high permeability is selected for the gas zone.

The simulation starts assuming both zones are producing at a steady state. As shown in Figure 7, from time zero to hour 1, the oil zone produces only oil, and the gas zone produces only gas. At hour 1, the wellhead choke is closed. The oil production from the oil layer (the solid black curve) then starts decreasing, however, it doesn't cease. In the meantime, the production from the gas zone turns to negative for both the gas and the oil phase. This implies that some of the oil produced from the oil zone together with its associated gas is injected to the gas zone. On reopening the wellhead choke at hour 6, the injected oil is produced back as a peak given by the solid red curve in the figure.

Due to the high permeability of the gas zone, the injected oil is flushed out very quickly by the gas. However, we do see in some other examples, that it can take much longer time for the oil to be driven out when the permeability is low, which can also significantly reduce the relative permeability to the gas phase in the near-wellbore region, thus, results in a long term low gas production.

Application in a well testing case

Dynamic wellbore/reservoir integrated simulation is a valuable tool for designing and optimizing transient well tests. In particular, in a hostile downhole environment where measurements may not be cost-effective or reliable, the ability to estimate BHP accurately from surface measurements is an invaluable asset. In addition, one can also get more abundant information from the simulation of a validated model to assist the well testing interpretation, e.g. using the validated model to obtain accurate downhole multiphase rates to optimize future application of deconvolution techniques.

As an attempt on this, the integrated model described in this paper is employed to simulate a well testing process for an offshore appraisal gas well. The main task here is to build a numerical wellbore/reservoir system to match the well testing data so that it can be used for further "virtual" testing purposes.

The appraisal well was drilled to confirm the extension and volume range of the reservoir. It was completed at the base of the productive zones. Wireline logs/cores/pressure and fluid samples were acquired. Annular pressure operated DST tools with packer and 4.5" TCP guns were run on production test string (3.5" OD, 2.725" ID) premium tubing.

The main test string data gathering components were (see Figure 8):

- Downhole shut-in valve to minimize the impact of wellbore effects on recorded reservoir pressure data.
- Surface pressure readout facility to minimize rig time by reducing the buildup period to be the minimum required to obtain significant reservoir pressure data.
- Quartz memory pressure gauges located on the test string as follows:
  a. Upper gauge: above the downhole shut-in valve
  b. Middle gauge: below the downhole shut-in valve
  c. Bottom gauge: below bottom perforations

The explored reservoir consists of 5 stacked zones. The early-time reservoir parameters like pressure and permeability were used to compose the reservoir model.

The testing program was divided into the following steps as shown in Figure 9:

Cleanup period. This initial flow period was designed to lift completion fluid out of the annulus below the packer and to clean up the formation in the vicinity of the well bore that has been affected by invasion of drilling fluids. Production data at surface will be recorded as a function of time and will be used to define the duration of the clean-up period.

Initial buildup period. This is to determine the initial reservoir pressure and to restore reservoir equilibrium before embarking on the main flow period.

First multiflow period. Flow after flow at two stabilized flow rates to determine inflow performance relationship between downhole pressures and gas production rates, in particular to calculate the rate dependent skin factor.

First main buildup period. Record the pressure and temperature reservoir response to gas production during main flow period to determine reservoir characteristics.

Second multiflow period. Flow after flow at three stabilized flow rates to determine inflow performance relationship between downhole pressures and gas production rates.

Second main buildup period. Record the pressure and temperature reservoir response to gas production during main flow period to determine reservoir characteristics.

After running the test string into the hole and setting the test packer, the well was perforated and opened to flow at surface. Figure 8 shows the initial conditions prior to the cleanup. At the end of the initial buildup, the well was opened downhole first and at the surface manifold later for the first flow test. The initial well shut-in was performed downhole as planned. When trying to shut-in the well again for the first main buildup test, the downhole shut-in valve was stack-open, therefore, the well was shut-in at surface only using the manifold choke. From then on all shut-in and start-up well operations were performed from surface.

Modeling

The well is modeled from its bottom to the manifold on the MODU with the major valves included. At the outlet, measured manifold pressure downstream of the choke is used as the boundary condition, see Figure 10. At the well bottom, the near-wellbore reservoir model for the five production zones is connected to the corresponding numerical sections of the well. Below the inflow sections, there is a rat hole containing the bottom gauge. A linear formation temperature profile in the vertical direction is assumed as the outer boundary for the wellbore heat transfer calculations. For the riser between the subsea wellhead and the MODU, a linear sea water temperature profile is assumed, with the sea current velocity considered when calculating the outer wall heat transfer coefficient. The tubing wall, the completion fluid in the annulus, the casing wall, and a certain thick of formation are modeled as composite wall layers with given thermal properties for each layer.

The reservoir model is built based on the forecasted information received. A cylindrical reservoir of 150 meter in radius is modeled with five numerical layers, one layer for each zone. The given reservoir pressure and permeability for each zone are used. For each layer, the reservoir is assumed to be homogeneous. For other unavailable parameters, assumptions have to be made. As no water is produced at the sandface, the water saturation in the reservoir is assumed to be at its irreducible level. A homogenous porosity of 30% is assumed for all the layers. An artificial skin factor is applied to each layer when calculating the sandface flowrate. However, no rate-dependant skin is considered as it has not been implemented in the current version of the reservoir model.

Simulation and tuning

The matching targets are the pressure signals from the three downhole gauges. The matching is done by a trial-and-error through tuning the skin factor prior to each run. The other parameter such as reservoir pressure and permeability are not touched during the whole matching process.

As shown in Figure 8, prior to the cleanup, the tubing string is filled with completion fluid below the packer and diesel above the packer, which means the well model should be able to handle the co-flow of mud and diesel with the reservoir fluid. The wellbore flow model[16,17] used in this work does have this capability; but the objective of this simulation study was to analyze the wellbore/reservoir interaction during the flow-after-flow and build-up tests with no inclusion of the clean-up period. Therefore, different initial conditions have to be assumed to kick off the simulation, which means no comparison can be made for the initial cleanup process and the early stage of the first multifluid period. So, when tuning the skin factor to match the measurements, the focus is set on the process from the late stage of the first multifluid period to the end of the testing.

Results and discussion

The comparison between the simulation results and the three downhole gauges' measurements are presented in Figure 11, Figure 12 and Figure 13, for upper, middle and bottom gauge respectively.

During the trial-and-error process, the tuning of the skin factor is based on the bottom gauge pressure measurements between 1500 and 2300 minutes without considering the other part of process. After only three rounds of trial-and-error, the results like in Figure 11, Figure 12 and Figure 13 can be achieved.

The simulation can almost perfectly match the bottom gauge measurements. But for the upper and middle gauge, the simulation gives a slower pressure buildup even though the final shut-in pressure can be matched in the end as shown by the trend after 6000 minutes for the last main buildup. One of the reasons for this slow pressure buildup could be due to the non-Darcy effect of the gas flow from the reservoir.

At the moment, the reservoir model used here can only simulate Darcy flow and the rate-dependent skin is not implemented yet. Therefore, the skin factor tuned under the high flow period (1500~2300 minutes) may not be suitable for low flow rates such as during the shut-in. In principle, when the flow rate goes down, the non-Darcy skin is also reduced, thus, it will slow down the flowrate decreasing, which may accelerate the buildup.

On the other hand, the increased pressure buildup for the upper and middle gauge does not necessary cause pressure over-shoot for the bottom, as a relative high gas rate may reduce the falling of liquid film and droplets, and as a consequence, reduce the hydrostatic pressure gradient. This means by considering the non-Darcy effect, the matching of pressure buildup for middle and upper gauge should be able to maintain the already perfect matching at the bottom gauge.

Other parameters such as the porosity can also affect the transient reservoir behavior. However, in order to keep the tuning process simple, the other parameters are not touched. Nevertheless only the skin factor is tuned, the matching results already look promising. But the possibility of getting a perfect match does exist by refining the trial-and-error through multi-parameter tuning.

Conclusions

A dynamic wellbore/reservoir model was built, tested, and applied to a well testing case. The wellbore model and the reservoir model selected for coupling are powerful and comprehensive in functionalities. The implicit numerical coupling scheme between the two models gives the required robustness and high speed for integrated transient simulations.

Testing results show that the integrated simulation can more accurately predict the well flow transients like shut-in/start-up and gas-lift casing heading than the IPR approach does. It can also simulate some scenarios such as dynamic coning and crossflow that can not be revealed by the IPR approach.

The integrated model is also adequate in modeling and simulating the transient behaviors encountered during well testing. The application in this paper demonstrates that an integrated model can be very easily tuned to match the well testing data, and therefore be used as a tool for planning well testing, assisting well test interpretation, and estimating BHP when downhole hardware measurements are not applicable.

Acknowledgement

This work is a development of the HORIZON project that is jointly sponsored by Statoil, Hydro, Shell, ExxonMobil, Chevron, and ENI. The authors would like to thank all the sponsors for their encouragement and permission to publish this paper.

Abbreviations

IPR = Inflow Performance Relationship
BHP = Bottom Hole Pressure
TPR = Tubing Performance Relationship
PVT = Pressure Volume Temperature
GOR = Gas Oil Ratio
SC = Standard Condition
DST = Drill Stem Testing
TCP = Tubing Conveyed Perforating
TVD = True Vertical Depth
MODU = Mobile Offshore Drilling Unit

Unit conversion factors

m x 2.54	E-02 = in
m^2 x 9.86	E-16 = mDarcy
Pa x 1.4504	E-04 = psi
Pa x 1.0	E-05 = bar

References

1. Gaspari, E.F., Oliveira, G.P.H.A., Monteiro, M.R.B. and Dourado, R.J.: "Evaluating Transient Multiphase Model Performance for the Brazilian Offshore Environment", OTC paper 17956, presented at the Offshore Technology Conference held in Houston, Texas, USA, 1-4 May, 2006.
2. Winterfield, P.H.: "Simulation of Pressure Buildup in a Multiphase Wellbore/Reservoir System", SPE paper 15534, presented at the SPE Annual Technical Conference and Exhibition held in New Orleans, USA, 25-26 March, 1986.
3. Stone, T.W., Edmunds, N.R. and Kristoff, B.J.: "A Comprehensive Wellbore/Reservoir Simulator", SPE paper 18419, presented at the SPE Symposium on Reservoir Simulation in Houston, USA, 6-8 February, 1989.
4. Almehaideb, R.A., Aziz, K. and Pedrosa Jr., O.A.: "A Reservoir/Wellbore Model for Multiphase Injection and Pressure Transient Analysis", SPE paper 17941, presented at the SPE Middle East Oil Technical Conference and Exhibition, Manama, Bahrain, 11-14 March, 1989.
5. Siu, A., Li, Y.K., Nghiem, L. and Redford, D.: "Numerical Modeling of a Thermal Horizontal Well", CIM/SPE paper 90122, the CIM/SPE meeting, Calgary, 1990.
6. Hasan, A.R., Wang, X. and Kabir, C.S.: "A Transient Wellbore/Reservoir Model for Testing Gas Wells in High Temperature Reservoirs", SPE paper 28402, presented at the SPE Annual Technical Conference and Exhibition held in New Orleans, USA, 25-28 September, 1994.
7. Kabir, C.S., Hasan, A.R., Jordan, D.L. and Wang, X.: "A Transient Wellbore/Reservoir Model for Testing Gas Wells in High Temperature Reservoirs, Part II Field Application", SPE paper 28403, presented at the SPE Annual Technical Conference and Exhibition held in New Orleans, USA, 25-28 September, 1994.
8. Hasan, A.R., Kabir, C.S. and Wang, X.: "Development and Application of a Wellbore/Reservoir Simulator for Testing Oil Wells", SPE paper 29892, presented at the SPE Middle East Oil Show held in Bahrain, 11-14 March, 1995.
9. Su, H-J. and Lee, S.H.: "Modeling Transient Wellbore Behavior in Horizontal Wells", SPE paper 29961, presented at the International Meeting on Petroleum Engineering held in Beijing, PR. China, 14-17 November, 1995.
10. Hasan, A.R., Kabir, C.S. and Wang, X.: "Wellbore Two-Phase Flow and Heat Transfer during Transient Testing", SPEJ 3 (2), 174-180, 1998.
11. Fan, L., Lee, W.J. and Spivey, J.P.: "Semi-Analytical Model for Thermal Effect on Gas Well Pressure-Buildup Tests", SPE paper 56612, presented at the SPE Annual Technical Conference and Exhibition held in Houston, USA, 3-6 October, 1999.
12. Maggard, J.B., Wattenbarger, R.A. and Scott, S.L.: "Modeling Plunger Lift for Water Removal from Tight Gas Wells", SPE paper 59747, presented at the SPE/CERI Gas Technology Symposium held in Calgary, Alberta Canada, 3-5 April, 2000.
13. Sturm, W.L., Belfroid, S.P.C., van Wolfswinkel, O., Peters, M.C.A.M. and Verhelst, F.J.P.C.M.G.: "Dynamic Reservoir Well Interaction", SPE paper 90108, presented at the SPE Annual Technical Conference and Exhibition held in Houston, USA, 26-29 September, 2004.
14. Ballard, A.L., Adeyeye, D., Litvak, M., Wang, C.H., Stein, M.H., Cecil, D. and Dotson, B.D.: "Predicting Highly Unstable Tight Gas Well Performance", SPE paper 96256, presented at the SPE Annual Technology Conference and Exhibition held in Dallas, USA, 9-12 October, 2005.
15. Izgec, B., Kabir, C.S., Zhu, D. and Hasan, A.R.: "Transient Fluid and Heat Flow Modeling in Coupled Wellbore/Reservoir Systems", SPE paper 102070, presented at the Annual Technical Conference and Exhibition held in San Antonio, USA, 24-27 September, 2006.
16. Bendiksen, K.H., Malnes, D., Moe, R. and Nuland, S.: "The Dynamic Two-Fluid Model OLGA: Theory and Application", SPEPE, 171, May 1991.
17. Nossen, J., Shea, R. and Rasmussen J.: "New Developments in Flow Modeling and Field Data Verification", 2nd North American Conference on Multiphase Technology, Banff, Canada, 21-23 June, 2000.
18. Sagen, J., Sira, T., Ek, A., Selberg, S., Chaib, M. and Eidsmoen, H.: "A Coupled Dynamic Reservoir and Pipeline Model – Development and Initial Experience", 13th International Multiphase Conference on Multiphase Production Technology 07', Edinburg, UK, 13-15 June, 2007.
19. Chupin, G., Hu, B., Haugset, T., Sagen, J. and Claudel, M.: "Integrated Wellbore/Reservoir Model Predicts Flow Transient in Liquid-Loaded Gas Wells", SPE paper 110461, presented at the SPE Annual Technical Conference and Exhibition held in Anaheim, USA, 11-14 November, 2007.
20. Asheim, H.: "Analytical Solution of Dynamic Inflow Performance", SPE paper 63307, presented at the SPE Annual Technical Conference and Exhibition held in Dallas, USA, 1-4 October, 2000.
21. Hasan, A.R. and Kabir, C.S.: "Discussion of Transient Dynamic Characteristics of the Gas-Lift Unloading Process", SPE 57711, SPE Journal 4 (3), pp302-303, 1999.

Table 1 Basic input information for Case 1.

Well depth	3000 m
Tubing size	6.75 in
Wellhead choke	6 in
Pressure downstream wellhead choke	80 bara
Drainage boundary pressure	300 bara
Payzone thickness	10 m
Reservoir temperature	70 °C
Reservoir formation porosity	0.2
Reservoir formation permeability	20 mDarcy
Liquid density of reseroir fluid at SC	838.2 kg/m^3
Gas density of reservoir fluid at SC	1.02 kg/m^3
GOR	204 Sm^3/Sm^3
Bubble pressure at reservoir temperature	225 bara

Table 2 Basic input information for Case 2.

Well depth	2048 m
Tubing size	5 in
Casing size	10 in
Wellhead choke	2.75 in
Gas-lift orifice size	0.5 in
Payzone thickness	50 m
Pressure downstream wellhead choke	60 bara
Drainage boundary pressure	175 bara
Reservoir temperature	70 °C
Reservoir formation porosity	0.25
Reservoir formation permeability	40 mDarcy

Table 3 Basic input information for Case 3.

Well depth (from seabed)	1375 m
Tubing size	4.5 in
Seabed flowline length	8125 m
Flowline diameter	8.75 in
Riser depth	1375 m
Riser diameter	6 in
Wellhead choke	2.75 in
Riser outlet pressure	80 bara
Gas cap thickness	30 m
Oil zone thickness	60 m
Drainage boundary pressure	300 bara
Reservoir temperature	70 °C
Reservoir formation porosity	0.2
Reservoir formation permeability	10 mDarcy

Table 4 Basic information for Case 4.

Well depth	3000 m
Gas layer depth	2375 m
Thickness of gas layer	20 m
Thickness of oil layer	20 m
Tubing size	8.25 in
Wellhead choke	6 in
Pressure downstream wellhead choke	20 bara
Oil layer drainage boundary pressure	180 bara
Gas layer drainage boundary pressure	130 bara
Oil layer reservoir formation porosity	0.28
Gas layer reservoir formation porosity	0.28
Oil layer reservoir formation permeability	200 mDarcy
Gas layer reservoir formation permeability	1 Darcy

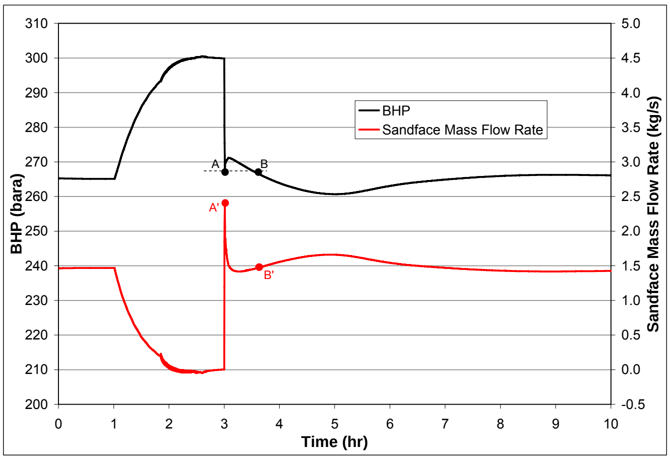

Figure 1 Variation of BHP and sandface mass flow rate during well shut-in and start-up, Case 1.

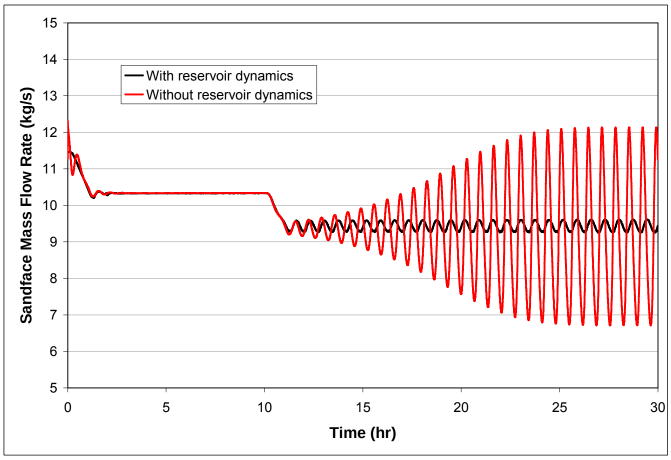

Figure 2 Comparison of the onset of casing heading: with and without considering reservoir dynamics, Case 2.

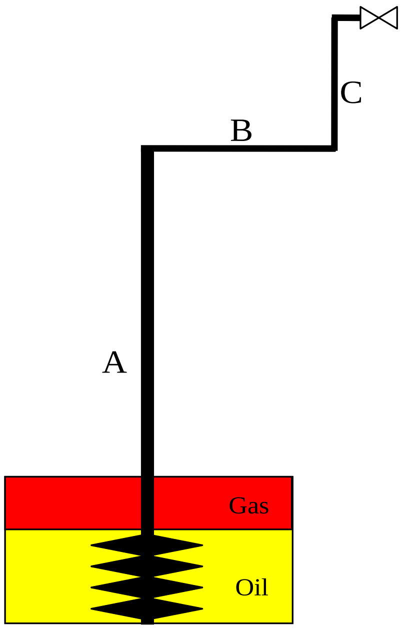

Figure 3 Schematic drawing of the reservoir-well-flowline system simulated in Case 3.

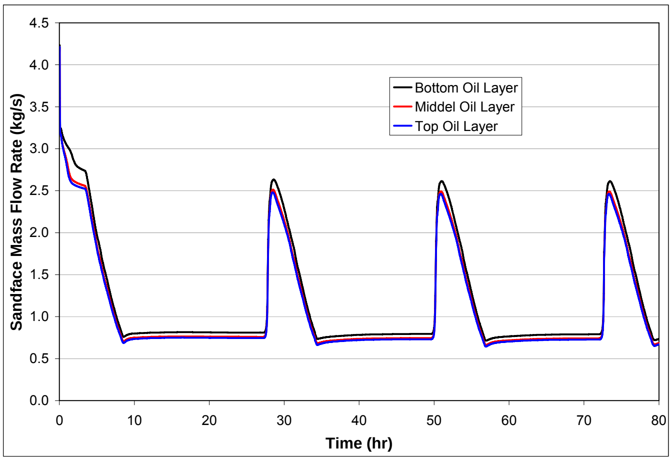

Figure 4 Sandface oil mass flow rate without considering dynamic gas coning effect, Case 3.

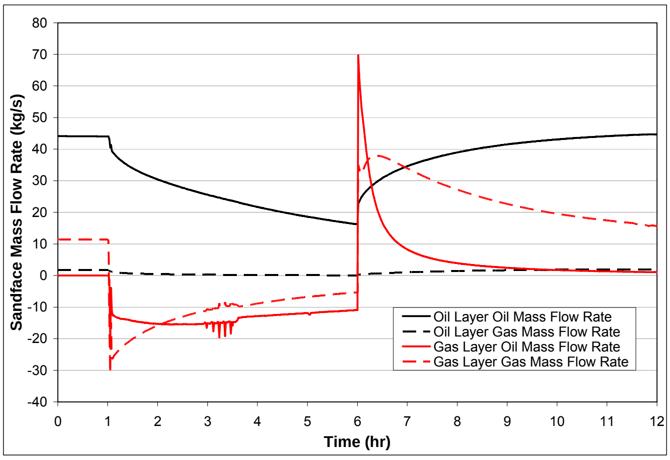

Figure 7 Crossflow between upper and lower layer during shut-in/start-up of a two layer well, Case 4.

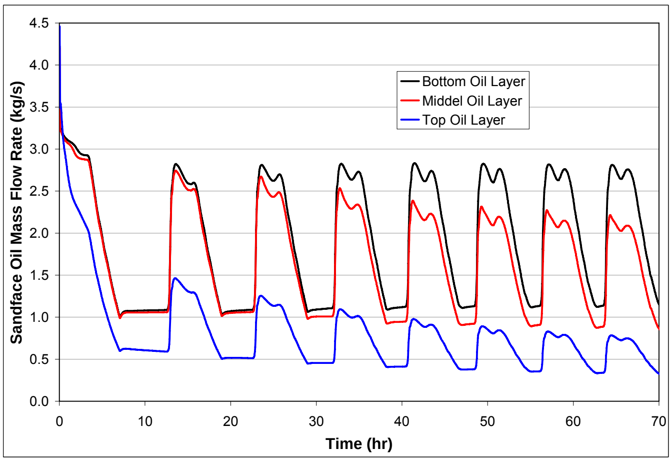

Figure 5 Sandface oil mass flow rate considering dynamic gas coning effect, Case 3.

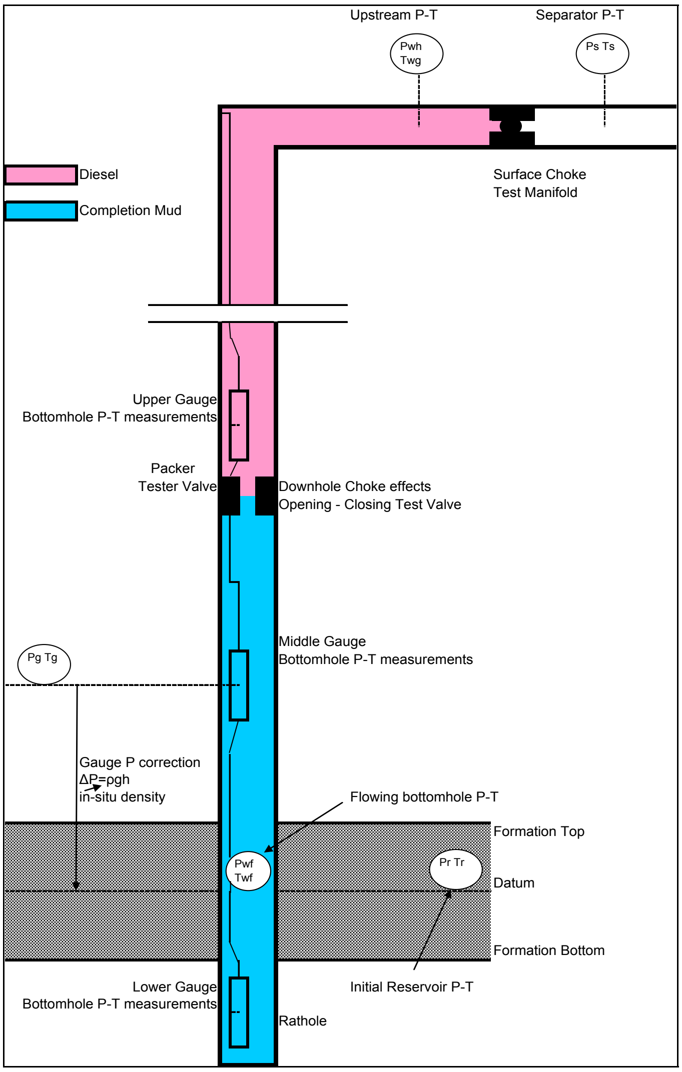

Figure 8 Well test equipment, gauge location, and initial conditions.

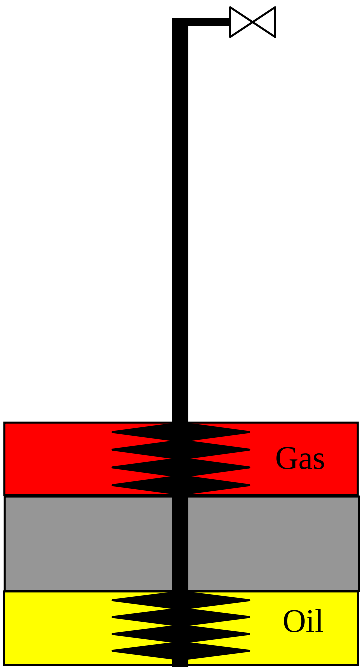

Figure 6 Schematic drawing of the reservoir-well system simulated in Case 4.

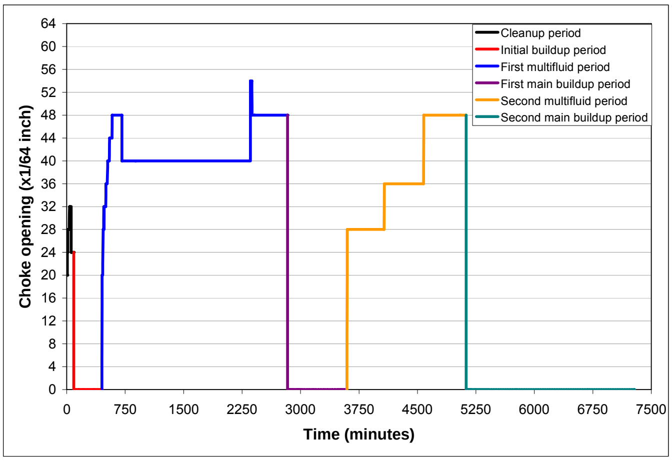

Figure 9 DST flow sequence and timing.

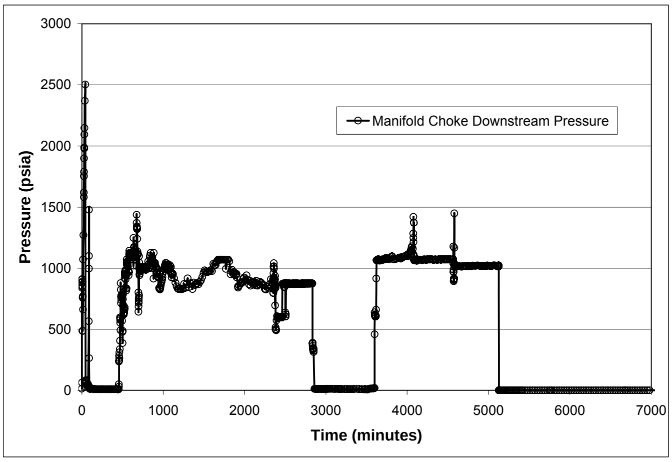

Figure 10 Manifold choke downstream pressure as outlet boundary condition for simulation.

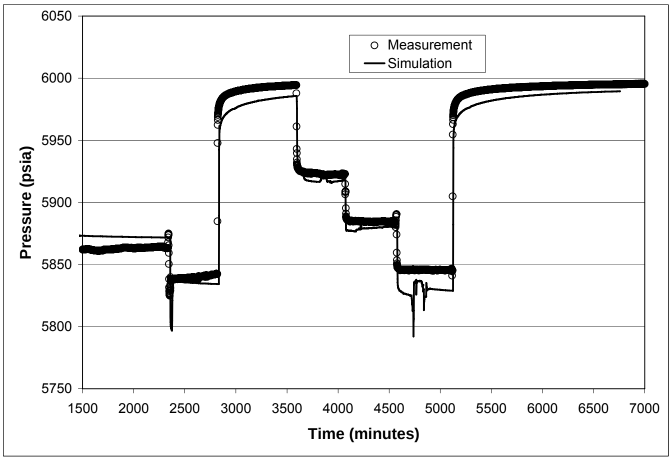

Figure 11 Upper gauge pressure: measurement vs. simulation.

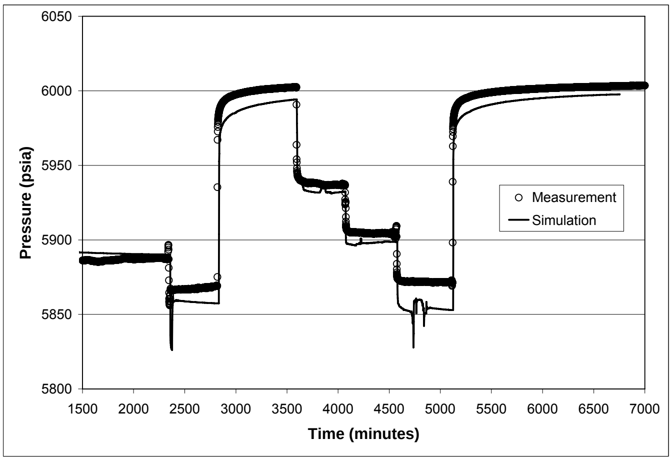

Figure 12 Middle gauge pressure: measurement vs. simulation.

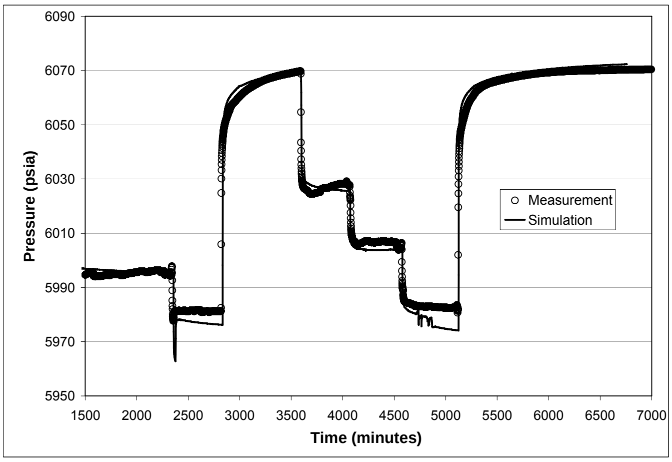

Figure 13 Bottom gauge pressure: measurement vs. simulation.